UDK 537.226.3:661.687
Original scientific article/Izvirni znanstveni članek

ISSN 1580-2949
MTAEC9, 56(1)79(2022)

DIELECTRIC LOSS OF Si_2N_2O AND THE INFLUENCE OF Li ON ITS PROPERTIES

DIELEKTRIČNE IZGUBE Si_2N_2O IN VPLIV Li NA NJEGOVE LASTNOSTI

Yong Yang[1], Ming He[2], Ting Zhang[1*], Meng-qiang Wu[3]

[1]Department of Biomedical Engineering, School of Big Health and Intelligent Engineering, Chengdu Medical College, Chengdu 610500, China
[2]Electronic Engineering Institute, Chengdu Technological University, Chengdu, China
[3]State Key Laboratory of Electronic Thin Films and Integrated Devices, University of Electronic Science and Technology of China, China

Prejem rokopisa – received: 2021-12-03; sprejem za objavo – accepted for publication: 2022-01-05

doi:10.17222/mit.2021.334

The dielectric losses of Si_2N_2O, studied theoretically and experimentally up to 1573 K at 10 GHz, demonstrated an increase above 1000 K due to the impurity conduction losses, because of the small Li activation energy. Calculations based on the first-principles theory were performed to obtain the density of states. The optical and elastic properties of Si_2N_2O doped with a 4.8 % molar fraction of Li were modeled using a plane-wave pseudopotential method to investigate the effect of Li incorporation into Si_2N_2O. The polycrystalline static dielectric constants of Si_2N_2O increased after it was doped with Li. We also provided the optical properties of silicon nitride compounds to be used as references. The calculated elastic constants of pure and Li-doped Si_2N_2O indicated that the elastic modulus of the Li-doped Si_2N_2O was smaller than that of the pure Si_2N_2O. Additionally, Li-doped Si_2N_2O crystals were more brittle than the pure forms. Theoretical analyses of the dielectric losses and first-principles calculations emphasized that to consider Li-doped Si_2N_2O materials for applications, the dielectric losses and Li contents should be carefully optimized, since these factors also affect the conductivities of these materials.

Keywords: Si_2N_2O, dielectric loss, high temperature, Li doping

Dielektrične izgube silicijevega oksinitrida (Si_2N_2O), določene do 1573 K pri 10 GHz naraščajo nad 1000 K zaradi nečistoč, ki zavirajo prevodnost oz. zaradi majhne aktivacijske energije litija (Li). Avtorji članka so z namenom določitve gostote stanj izvedli izračune, ki temeljijo na teoriji prvega načela. Pri raziskavi vpliva dodatka Li na Si_2N_2O, so avtorji s pomočjo ravninsko valovne psevdo-potencialne metode, modelirali optične in elastične lastnosti Si_2N_2O dopiranega s 4,8 mol. % Li. Polikristalinične statične dielektrične konstante Si_2N_2O so naraščale po dopiranju z Li. Avtorji so prav tako določili referenčne optične lastnosti spojin silicijevega nitrida. Izračunane elastične konstante čistega in z Li dopiranega Si_2N_2O kažejo, da so elastični moduli z Li dopiranega Si_2N_2O manjši od tistih, ki jih ima čisti Si_2N_2O. Dodatno so kristali z Li dopiranega Si_2N_2O bolj krhki kot kristali nedopiranega (čistega) Si_2N_2O. Teoretične analize dielektričnih izgub in izračuni na temelju teorije prvega načela potrjujejo uporabnost z Li dopiranega Si_2N_2O. Pri tem morajo biti dielektrične izgube in vsebnost Li skrbno optimizirane, ker je od teh faktorjev odvisna tudi prevodnost teh materialov.

Ključne besede: Si_2N_2O, dielektrične izgube, visoke temperature, dopiranje z Li

1 INTRODUCTION

Electromagnetic-wave-transparent materials can transmit microwaves and are widely used on carrier rockets, airships, missiles, and return satellites.[1] Silicon oxynitride (Si_2N_2O) possesses excellent thermal shock resistance, good mechanical properties and dielectric behavior. Thus, this material could be used as an excellent radome material, as well as for applications related to high-temperature electronic insulators, nuclear reactions and solid electrolytes.[2–4] Additionally, silicon oxynitride films (SiO_xN_y) possess other favorable properties, including a controllable refractive index and an adjustable stress, which allow this material to be used in optical devices as wave-guide materials, as well as for applications related to non-volatile memories.[5,6]

Most recent research efforts dedicated to dielectric ceramic materials focus on their preparation and composition.[7–9] As a result, new computational methods were developed to understand and analyze the compositions, structures and other related properties of these materials. Such methods are not limited by the experimental constraints, including material selection and preparation techniques, which significantly reduced the difficulties and costs associated with the experimental research of these materials. One of the specific examples of the theoretical analysis of Si_2N_2O electronic structure performed by first-principles calculations includes the work by Zhen-long Lv et al.[10] They modeled the vibrational and dielectric properties, the strength and the deformation mechanism of Si_2N_2O. However, they barely discussed any analysis of the refractive index, the losses and the conductivity of Si_2N_2O.

Recently, a new method of Si_2N_2O synthesis involving its doping with lithium oxide was introduced. The dielectric constant and the loss of the resulting Si_2N_2O were equal to 6.17 and 0.0008, respectively.[11] Such excellent dielectric properties would make Si_2N_2O very

*Corresponding author's e-mail:
flyrain68@126.com (Ting Zhang)

useful as a high-temperature electronic insulator for reactors, solid electrodes, etc. However, the mechanism of Si_2N_2O dielectric losses as a function of temperature is not evident. Therefore, this paper is dedicated to a theoretical and experimental analysis of the microwave dielectric losses of Si_2N_2O in the range 302–1573 K. We also report on how the level of Li doping affected the properties of the Si_2N_2O.

2 COMPUTATIONAL DETAILS

Pure Si_2N_2O was selected to calculate the losses at the microwave frequency (10 GHz). According to literature reports, the measurements were performed using cavity perturbation in the range 302–1573 K.[12] Very low dielectric losses were observed below 1000 K (**Figure 1a**). However, above 1000 K, some dielectric losses were observed as the temperature was increased, reaching 0.0135 at 1573 K. The dielectric losses at different frequencies are shown in **Figure 1b**. The total dielectric loss decreases with frequency, but to a lesser extent than with temperature.

The discussion below focuses on a theoretical analysis of this phenomenon. The main mechanisms of the dielectric loss are:

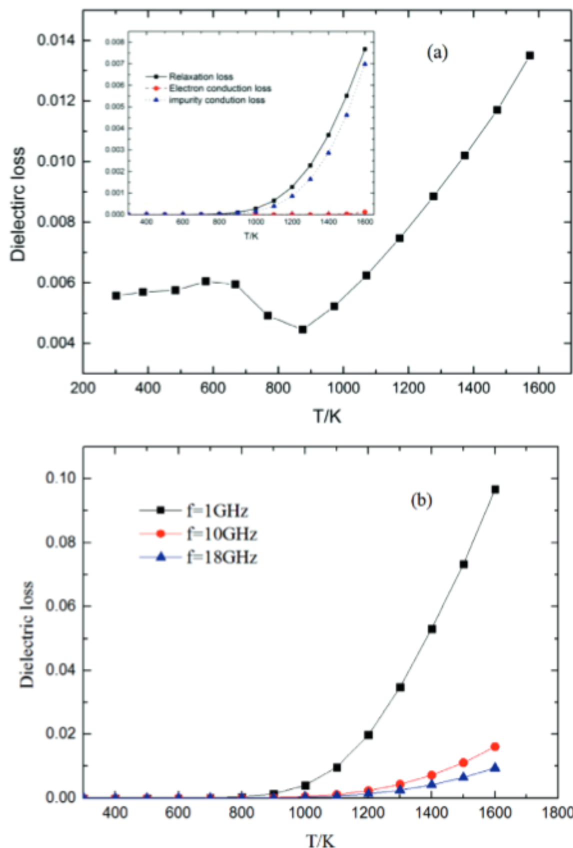

Figure 1: a) Experimental losses from 302K to 1573K, with the inset representing the ion conduction loss, the relaxation loss and electron conduction loss, and b) the calculated loss of Si_2N_2O at different frequencies

1) Slow polarization (such as thermionic polarization and thermal transformation polarization, which are closely related to thermal motion).
2) Conductivity loss, including electronic and ionic conductivity losses.
3) Resonance effect caused by the vibration of atoms, ions or electrons (this effect occurs in the infrared-to-ultraviolet optical frequency range).
4) A particular loss form related to the structural relaxation of the medium/structural loss (the less dense is the structure, the greater is the loss).

Because the frequency range of Si_2N_2O is in the microwave band, the frequency is much smaller than the optical frequency, so the resonance effect of atoms, ions or electrons cannot be considered. In addition, the impurity content of Si_2N_2O is small. Thus, structural defects and crystallinity losses were not considered as contributors to the dielectric losses. Therefore, the overall dielectric loss was considered as the sum of the relaxation and conductance losses.

Typically, the dielectric loss can be expressed as Equation (1):

$$\tan\delta = \frac{\varepsilon''}{\varepsilon'} + \frac{\gamma}{\omega\varepsilon'\varepsilon_0} \tag{1}$$

where γ is the sum of the electron (γ_e) and ionic (γ_{im}) conductivities of the Si_2N_2O impurities :

$$\gamma = \gamma_e + \gamma_{im} \tag{2}$$

The electron conductivity originates from the movement of free electrons, while the ionic conductivity is caused by impurities and defect leaks in the dielectric material. The contribution of other types of conductivities is negligible. The ionic conductivity can also be expressed in terms of the activation energies (U) of the impurities:

$$\gamma_{im} = \gamma_0 e^{-\frac{U}{kT}} \tag{3}$$

where k and T are the Boltzmann constant and the temperature, respectively, and γ_0 is a pre-exponential factor. Because Li_2O is commonly used as a dopant for ceramics, the impurities mainly originate due to the presence of Li. In this case, the activation energies of these impurities can be expressed using the Anderson-Stuart model, typically applied to glasses:[13]

$$U = E_b + E_s = \frac{\beta z z_0 e^2}{\gamma(r + r_0)} + 4\pi G r_D (r - r_D) \tag{4}$$

where G is the shear modulus of the doped material, z (and z_0), r (and r_0) are the charges and the radius of impurity (and negative) ions, respectively, γ is the atom deformability and is equal to the dielectric constant, which can be obtained from reference,[14] r_D is the effective radius of the doorway. This model can also describe dense systems if the 4π factors of the strain energy (E_s) are substituted by other values. In addition, the electri-

cal conductivity can be calculated by the solid-state relaxation Equation (5):[15]

$$\gamma_e = \frac{n_h e^2 v_h}{m_h(\omega^2 + v_h^2)} + \frac{n_e e^2 v}{m_e(w^2 + v_e^2)} \quad (5)$$

where n, m and e are the concentration of the charge carriers, the mass, and the electron charge, respectively, and v is the carrier collision frequency. The subscripts h and e denote holes and electrons, respectively. The phonon and impurity scattering can be expressed as Equation (6):

$$v = cT^{2/3} + dT^{-2/3} \quad (6)$$

where c and d are the phonon and impurity scattering constants, respectively.

Semiconductor-physics theory states that the electron density can be expressed as:

$$n_e = 2\left(\frac{2\pi k_0 T}{h^2}\right)^{3/2}(m_e m_h)^{3/4} \exp\left(-\frac{E_g}{2kT}\right) \quad (7),$$

where E_g is the bandgap equal to $E_g = E_{g0} - \eta(T-T_0)$, where E_{g0} is the room-temperature bandgap of Si_2N_2O equal to 5.97 eV, and η is the bandgap temperature coefficient.[16]

Assuming $m_e = m_h$, $n_e = n_h$, $v_e = v_h$, $d = 0$, and $\omega < v_e$, the electron conductivity can be expressed by combining Equations (5) to (7) as follows:

$$\gamma_e = \frac{4e^2\sqrt{m_e}\left(\frac{2\pi k}{h^2}\right)^{3/2} T^{3/2} \exp\left(-\frac{E_g}{2kT}\right)}{v_e} \quad (8)$$

Thus, the total loss depends on the relaxation ($\tan\delta_\beta$), electronic conduction ($\tan\delta_{ce}$) and defect (or impurity) ionic conduction ($\tan\delta_{rim}$) losses. The expressions below are calculated by combining Equations (1) to (8):

$$\tan\delta_\beta = \frac{\varepsilon''}{\varepsilon'} \quad (9)$$

$$\tan\delta_{ce} = \frac{4e^2\sqrt{m_e}\left(\frac{2\pi k}{h^2}\right)^{3/2} T^{3/2} \exp\left(-\frac{E_g}{2kT}\right)}{\omega\varepsilon'\varepsilon_s v_e} \quad (10)$$

$$\tan\delta_{rim} = \frac{p_{im}\rho_0 N_A q^2 \delta^2 v}{6kTm_{im}\omega\varepsilon_0\varepsilon'} e^{\left(-\frac{U}{kT}\right)} \quad (11)$$

3 RESULTS AND DISCUSSION

3.1 Dielectric losses of Si_2N_2O

The total microwave loss of Si_2N_2O consists of the relaxation, electronic conductivity and impurity ion losses. The theoretically obtained relaxation, electron conduction, and ionic conduction losses are shown in the inset of **Figure 1a**. The relaxation and impurity-ion conductance losses increase significantly with temperature and then increase exponentially above 1000 K. The contribution of the relaxation losses is the largest because the electrons and defects are not as active at low temperatures. As the temperature increases, the contribution of the impurity ions increases, while the influence of the electrons on the total dielectric loss remains small. Above 1000 K, the total dielectric loss is primarily composed of the relaxation and impurity losses. This may be because the conduction loss of the impurities is mainly affected by the activation energy U (see Equation (11)). The activation energy, in turn, is affected by its dissociation and migration energies. However, the dissociation energy decreases, and the migration energy increases as the ion radius increase. When the ion radius is small, the close association between the ion and the oxygen vacancy results in a higher dissociation energy. At the same time, the smaller is the resistance, the smaller is the migration energy. Typically, the activation energies of the monovalent metal ions (e.g., Li^+, Na^+, and K^+) are lower than the divalent and trivalent ions (e.g., Mg^{2+} and Al^{3+}) because the smaller the sizes, the easier is the transport and the higher is the conductivity. As shown in **Figure 2**, Li_2O impurity can create "fast ions" because it causes the formation of "open" structures, which increase the conductivity and ion losses. In comparison, other impurities, such as Ca^{2+}, are "slow", because their larger ion radii hinder their transport. Thus, their contribution to the overall electrical conductivity is negligible.

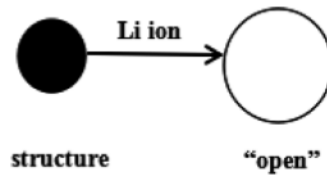

Figure 2: Influence of Li on the structure of Si_2N_2O

3.2 Effect of Li doping on the properties of Si_2N_2O

Because of the specifics of the synthesis and preparation process, Si_2N_2O always contains different concentrations of residual impurities, such as Li_2O.[14] These impurities could affect the dielectric behavior and mechanical properties of Si_2N_2O; therefore, their effect at high temperatures and on the high-frequency properties of Si_2N_2O needs to be studied. Our previous work showed that a modified Clausius-Mossotti equation and an additivity rule obtained using first-principles calculations could predict the Si_2N_2O's dielectric properties.[14] This work also performed the first-principles calculations using the CASTEP code to understand the influence of Li incorporation into Si_2N_2O on the properties of the matrix.[17] We employed the Vanderbilt-type ultra-soft pseudopotential and gradient-corrected approximations (GGA). The plane wave energy cut-off and the Brillouin zone were set at 571 eV and 3 × 5 × 5 k-point meshes, respectively. The geometry optimization tolerance was 5×10^{-6} eV/atom. X-ray powder diffraction (XRD) data was used as a starting point for the geometry optimiza-

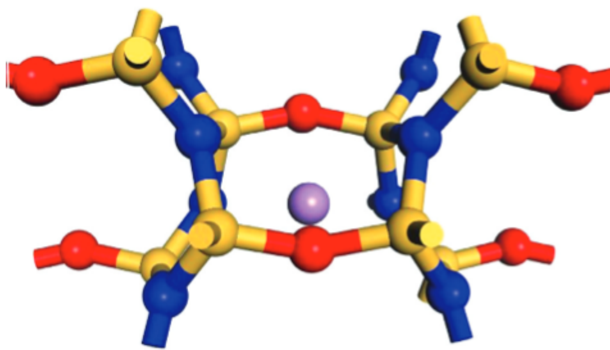

Figure 3: Crystal structure of Li-doped Si_2N_2O

tion. The Si_2N_2O has an orthorhombic structure with lattice constants equal to a = 0.8843 nm, b = 0.5437 nm and c = 0.4853 nm. Thus, Si_2N_2O building blocks are slightly distorted SiN_3O tetrahedral units linked, forming a three-dimensional network. Since the formation energy of Si substitution by Li is higher than that of the interstitial creation, these Li atoms could occupy the interstitial sites (**Figure 3**).[18] The BFGS minimization algorithm (proposed by Broyden, Fletcher, Goldfarb, and Shannon) was utilized to optimize the cell parameters and the atomic positions within a unit cell prior to any electronic structure calculations.

3.2.1 Effect of Li on the ground-state behaviors of Si_2N_2O

Figure 4 shows the electronic structure and property change as well as the electronic density of state (DOS) of Si_2N_2O with and without the presence of interstitial Li. **Figure 4a** shows the total (TDOS) and partial (PDOS)

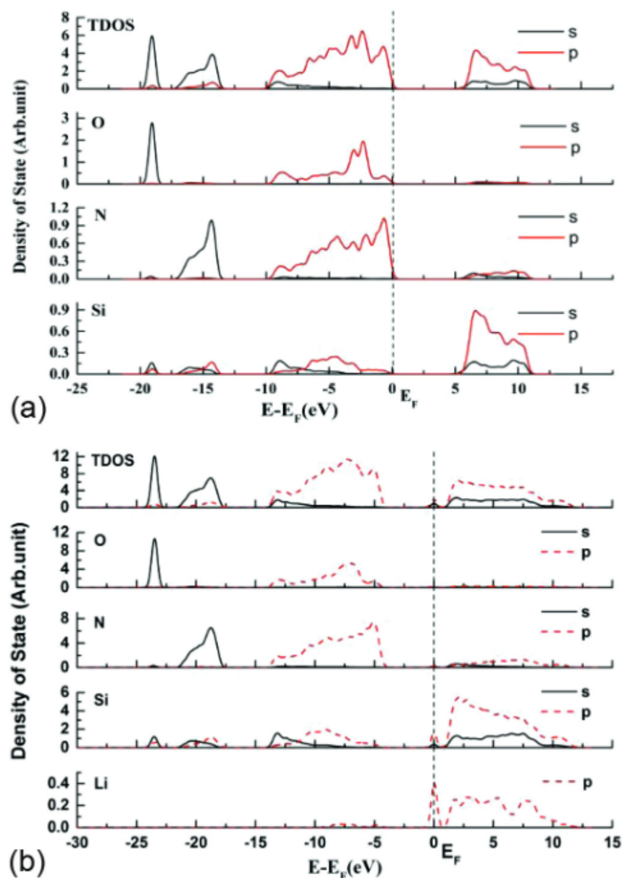

Figure 4: a) DOS and PDOS for Si_2N_2O and b) Li-doped Si_2N_2O (4.8 % molar fraction of Li)

DOS of pure silicon oxynitride. The valence bands accumulate as three groups (1.96; 4.43; 9.80) eV separated by

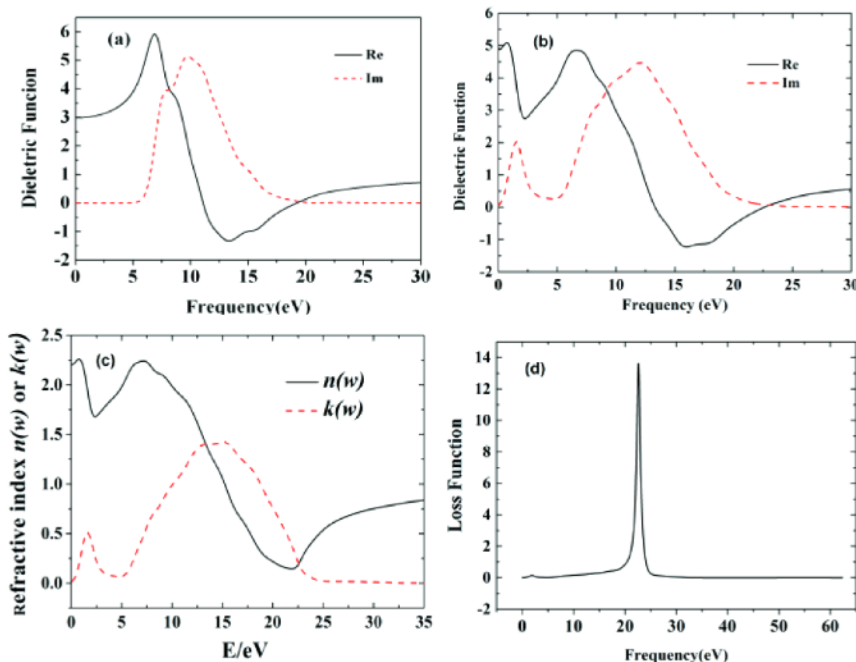

Figure 5: Calculated optical properties for Si_2N_2O and Li-doped Si_2N_2O

Table 1: Elastic constants for pure and Li-doped Si_2N_2O (4.8 % molar fraction of Li)

	C_{11}	C_{12}	C_{13}	C_{22}	C_{23}	C_{33}	C_{44}	C_{55}	C_{66}	B	G	E
Pure(this work)	330.4	104.3	66.4	278.2	51.5	329.2	135.5	62.3	75.0	152.3	92.4	242.4
Pure (calculated)[20]	316.0	81.3	51.5	241.6	31.0	320.7	139.1	59.7	76.2	132.7	97.1	234.2
Pure (exp.)[21]											93.1	221.6
Li-doped (this work)	254.3	34.2	44.1	201.7	26.8	283.1	105.1	50.3	44.9	105.5	82.3	196
Li-doped (exp.)[11]											85	192

0.05 eV and 2.12 eV gaps. The theoretical TDOS and PDOS of Si_2N_2O doped with 4.8 % molar fraction of Li are shown in **Figure 4b**. The bottom conductive bands of TDOS of the Li-doped Si_2N_2O shifted upwards, which made the corresponding bandgap narrower. The Fermi level of Li-doped Si_2N_2O at 2.12 eV is positioned higher than the bottom of the conductive band, which makes the Li-doped Si_2N_2O conductivity n-type. The donor states mainly originate from the Si 3p orbital, located at the bottom of the Si_2N_2O conductive band. Because there are no hybrid states between Li and O, their interaction can be considered ionic. We also found that the Li 2s state contributes to the top of the valance band and to the bottom of the conductive band. The band narrowing could be because of the intermixing between the Si 3p and Li 2s levels at the top of the valence band, which agrees with the literature.[19,20]

Figures 5a and **5b** shows the calculated dielectric function of pure and doped (with a 4.8 % molar fraction of Li) Si_2N_2O. The real and imaginary parts of the Si_2N_2O dielectric function showed peaks at 6 eV and 5 eV, respectively. The energy peaks are caused by the transfer of the excited electrons from the valence to the conduction band. The peaks of the real and imaginary parts of the Li-doped function were observed at 5 eV and 4.5 eV, respectively. **Figures 5a** and **5b** show the Si_2N_2O dielectric spectra before and after doping. The dielectric constant of the polycrystalline Li-doped Si_2N_2O (equal to 4.88 eV) is higher than that of the pure one, which agrees with the literature.[14,18] It also explains the observations of Tong et al.,[11] that the dielectric constant of polycrystalline Si_2N_2O increases as the residual Li content increases.

The optical properties of materials can be calculated from the dielectric functions $\varepsilon(\omega) = \varepsilon_1(\omega) + i\varepsilon_2(\omega)$. The imaginary part of the dielectric function is given as follows:

$$\varepsilon_2(\omega) = \frac{Ve^2}{2\hbar m^2\omega^2}\int d^3k\sum_{nn'}\left|<\vec{k}n|\vec{p}|\vec{k}n'\right|^2 \times \times f(\vec{k}n)(1-f(\vec{k}n'))\delta(E_{\vec{k}n}-E_{\vec{k}n'}-\hbar\omega) \quad (12)$$

where p is the momentum operator, e is the electronic charge, V is the volume, ω is the light frequency, m is the electronic mass, kn > and kn' > represent the wave functions of the conduction and valence bands (CB and VB, respectively) corresponding to the n-th and n'-th values with crystal momentum k, and $f(kn)$ is the Fermi distribution function.

The calculated reflective and loss spectra of Li-doped Si_2N_2O are presented in **Figures 5c** and **5d**. The material's optical properties can be presented in terms of the refractive-index data or damping constant/attenuation coefficients to demonstrate the electromagnetic wave attenuation within a material. The static refractive index $n(0)$ (equal to 2.21) changes proportionally with the energy in the transparency region and reaches its maximum in the ultraviolet region at 0.76 eV and its minimum (equal to 0.15) at 21.9 eV. The electron-energy-loss function $L(\omega)$ describes the energy loss of fast electrons passing through a material. Prominent peaks in $L(\omega)$ are associated with plasma oscillations. The corresponding bulk plasma frequencies ω(p) occur at $\varepsilon_2 < 1$ and $\varepsilon_1 = 0$. The $L(\omega)$ peak at 22.6 eV is equal to 13.6 (**Figure 5d**). These data could be used as a reference during the analysis of the optical properties of more complex SiO_xN_y-based materials.

3.2.2 Influence of Li on the elastic constants of Si_2N_2O

The nine independent elastic constants for pristine and Li-doped Si_2N_2O obtained theoretically and experimentally are shown in **Table 1**. The polycrystalline elastic modulus for Si_2N_2O can be calculated from these constants. However, minor deviations were observed for the C_{11}, C_{12}, C_{22}, and C_{23} constants of pure Si_2N_2O. Yet, the experimental Si_2N_2O shear modulus agrees with the calculated one. At the same time, the elastic modulus of Li-doped Si_2N_2O is smaller than that of pure Si_2N_2O, which is consistent with the experimental results.[11] Additionally, the B/G ratio can be used to estimate the material's ductility. Th B/G ratios of brittle materials, such as diamond, are typically equal to 0.83. The bulk and shear modulus calculated for pure and Li-doped Si_2N_2O yielded B/G values equal to 1.65 and 1.28, respectively. A smaller B/G ratio implies higher brittleness.

4 CONCLUSIONS

Si_2N_2O's dielectric losses were studied from room temperature to 1573 K. Our theoretical and experimental results demonstrated that the increase in the dielectric loss was mainly because of the impurity conduction losses, because of the small Li activation energy. The dielectric losses increased at higher impurity contents and temperature. In contrast, the dielectric loss decreased

with frequency. The dielectric losses increased as a function of frequency, but to a lesser degree than as a function of the temperature.

First-principles calculations of the density of states, as well as the optical and elastic properties of Li-doped Si_2N_2O, were performed using a method based on the plane-wave pseudopotential. The polycrystalline static dielectric constants of pure and Li-doped Si_2N_2O were equal to 3.0 eV and 4.88 eV, respectively, and agree with the literature. These optical data could be used as references during an analysis of the optical properties of more complex SiO_xN_y-based materials. The calculated elastic constants of Li-doped Si_2N_2O were smaller than those of the un-doped Si_2N_2O. Thus, the doped Li-doped Si_2N_2O is tougher. Li is an essential conductivity-enhancing component. Our theoretical analysis of the dielectric losses and first-principles calculations emphasized that the Li-doping concentration in Si_2N_2O systems needs to be controlled to achieve low dielectric losses at high temperatures.

Acknowledgements

This work was supported by the joint Foundationof ChenduMedical College – People's Hospital of Chengdu (grant. no. 2021LHPJ-03).

5 REFERENCES

[1] Z. L. Cheng, F. Ye, Y. S. Liu, Mechanical and dielectric properties of porous and wave-transparent Si_3N_4-Si_3N_4 composite ceramics fabricated by 3D printing combined with chemical vapor infiltration, J. Adv. Ceram., 8 (**2019**), 399–407, doi:10.1007/s40145-019-0322-8

[2] S. J. Lin, F. Ye, S. L Dong, Mechanical, dielectric properties and thermal shock resistance of porous silicon oxynitride ceramics by gas pressure sintering, Materials Science and Engineering: A, 635 (**2015**), 1–5, doi:10.1016/j.msea.2015.03.064

[3] Z. H. Zhou, Y. Lan, X. M. Li, Preparation and characterization of silicon oxynitride nanopowders via thermal explosion synthesis-Gravity separation strategy, Ceramics International, 47 (**2021**), 9287–9295, doi:10.1016/j.ceramint.2020.12.055

[4] Y. J. Li, D. H. Liu, B. Z. Ge, Fabrication of Si_2N_2O ceramic with silicon kerf waste as raw material, Ceramics International, 44 (**2018**), 5581–5586, doi:10.1016/j.ceramint.2017.12.203

[5] L. Y. Hang, W. G. Liu, J. Q. Xu, Effects of various substrate materials on microstructural and optical properties of amorphous silicon oxynitride thin films deposited by plasma-enhanced chemical vapor deposition, Thin Solid Films, 709 (**2020**), 138186, doi:10.1016/j.tsf.2020.138186

[6] A. Nagakubo, S. Tsuboi, Y. Kabe, Zero temperature coefficient of sound velocity in vitreous silicon oxynitride thin films, Appl. Phys. Lett., 114 (**2019**), 251905.1–251905.5, doi:10.1063/1.5098354

[7] H. Jin, Z. H.Yang, D. L. Cai, 3D printing of porous Si_2N^2O ceramics based on strengthened green bodies fabricated via strong colloidal gel, Materials & Design, 185 (**2020**), 108220.1–108220.9, doi:10.1016/j.matdes.2019.108220

[8] J. Li, C. Zhang, H. Liu, Structure, morphology, and microwave dielectric properties of $SmAlO_3$ synthesized by stearic acid route, J. Adv. Ceram., 9 (**2020**), 558–566, doi:10.1007/s40145-020-0394-5

[9] F. G. Huang, H. Su, Y. X. Li, Low-temperature sintering and microwave dielectric properties of CaMg1-xLi2xSi2O6 (x=0-0.3) ceramics, J. Adv. Ceram., 9 (**2020**), 471–480, doi:10.1007/s40145-020-0390-9

[10] Z. L. Lv, H. L. Cui, H. Wang, Vibrational and dielectric properties and ideal strength of Si_2N_2O ceramic from first principles, Ceramics International, 43 (**2017**), 10006–100012, doi:10.1016/j.ceramint.2017.05.014

[11] Q. F. Tong, J. Y. Wang, Z. P. Li, Low-temperature synthesis/densification and properties of Si_2N_2O prepared with Li_2O additive, J. Eur. Ceram. Soc., 27 (**2007**), 4764–4772, doi:10.1016/j.jeurceramsoc.2007.04.004

[12] E. Li, Z. P. Nie, G. F. Guo, Broadband measurements of dielectric properties of low-loss materials at high temperatures using circular cavity method, Progress In Electromagnetics Research, 92 (**2009**), 103–120, doi:10.2528/PIER09030904

[13] O. L. Anderson, D. A. Stuart, Calculation of activation energy of ionic conductivity in silica glasses by classical methods, J. Amer. Cera. Soc., 37 (**1954**), 573–580, doi:10.1111/j.1151-2916.1954.tb13991.x

[14] T. Zhang, M. Q. Wu, S. R. Zhang, Local electric field investigation of Si_2N_2O and its electronic structure, elastic and optical properties, Journal of Alloys and Compounds, 509 (**2011**), 1739–1743, doi:10.1016/j.jallcom.2010.10.026

[15] H. R. Li, Introduction to Dielectric Physics, University of Chengdu Electronic Science and Technology Press, Chengdu, 1990, 112

[16] W. Y. Ching, S. Y. Ren, Electronic structure of Si_2N_2O and Ge_2N_2O crystals, Physical Review B, 24 (**1981**), 5788–5795, doi:10.1103/PhysRevB.24.5788

[17] M. D. Segall, P. J. D. Lindan, M. J. Probert, First-principles simulation:ideas, illustrations and the CASTEP code, J. Phys. Condens. Matter., 14 (**2002**), 2717–2744, doi:10.1088/0953-8984/14/11/301

[18] B. Liu, J. Y. Wang, F. Z. Li, Effect of interstitial lithium atom on crystal and electronic structure of silicon oxynitride, J. Mater. Sci, 44 (**2009**), 6416–6422, doi:10.1007/s10853-009-3885-x

[19] W. Y. Ching, Electronic Structure and Bonding of All Crystalline Phases in the Silica-Yttria-Silicon Nitride Phase Equilibrium Diagram, J. Am .Ceram. Soc., 87 (**2004**), 1996–2013, doi:10.1111/j.1151-2916.2004.tb06352.x

[20] H. Z. Yao, L. Z. Ouyang, W. Y. Ching. Ab Initio Calculation of Elastic Constants of Ceramic Crystals, J. Am. Ceram. Soc., 90 (**2007**), 3194–3204, doi:10.1111/j.1551-2916.2007.01931.x

[21] P. Boch, J. C. Glandus, Elastic properties of silicon oxynitride, J. Mater. Sci., 14 (**1979**), 379–385, doi:10.1007/BF00589829